Non-Magnetic Ring Effect for Speed Increase of Solenoid Actuator

Baek-Ju Sung† and Eun-Woong Lee*

Abstract - To increase the operating speed of the solenoid actuator, this paper proposed a modified model using a non-magnetic ring, which is welded on the magnetic guide tube, and also presents the characteristic equations, results of Finite Element Method (FEM) analysis for magnetic flux distribution and density in magnetic flux paths, and computer simulation results for the dynamic characteristics of plunger motion according to the stroke and time variation. As well, we proved the non-magnetic ring effect by experiments using prototypes.

Keywords: Attraction Force, Solenoid Actuator, Non-Magnetic Ring, Plunger, Stationary Core

1. Introduction

The plunger speed of the solenoid actuator is affected by mass of the plunger, magnetic motive force, coil inductance, and spring constant of the return spring. These design factors are not independent but related with each other according to design characteristics. So, it is very difficult to change the value of any specific design factor for the purpose of increasing the plunger speed. If a designer changes the value of any design factor, the value of the other factors may be successively changed [1, 2].

For solving the difficulties of design, this paper proposed a modified model of a high-speed solenoid actuator using a non-magnetic ring, which is welded in the middle of the magnetic guide tube. The function of this model is to concentrate magnetic flux into the plunger.

This paper presents the characteristic equations of the solenoid actuator induced by use of the electrical equivalent circuit and mechanical equivalent circuit, the results of the Finite Element Method (FEM) analysis for all magnetic flux paths including the non-magnetic ring and its region, and the results of computer simulation for the dynamic characteristics of plunger motion according to the stroke and time variation. Especially, for more detailed analysis of non-magnetic ring effects, the FEM analysis is performed at some places determined by shaft directional position and length variation of the non-magnetic ring. Moreover, we proved the non-magnetic ring effect by experiments using prototypes.

† Dept. of Machinery Systems Reliability Research Center, Korea Institute of machinery & Materials. (sbj682@kimm.re.kr)
* Dept. of Electrical Engineering, Chungnam National University. (ewlee@cnu.ac.kr)
Received April 20, 2005 ; Accepted November 22, 2005

2. Equivalent Circuits and Characteristic Equations

2.1 Equivalent Circuit

Fig. 1 represents the sectional diagram of the proposed solenoid actuator in this study, which is composed of 6 parts such as stationary, plunger, yoke, rod, coil, and guide tube including the non-magnetic ring.

This model can be expressed as supply voltage V_s, resistance R, and inductance L from an electrical viewpoint and it also can be expressed as plunger mass M, frictional resistance R_v, and spring constant k from a mechanical viewpoint. Furthermore, we can summarize these as an electrical equivalent circuit and a mechanical equivalent circuit as indicated in Fig. 2 [1].

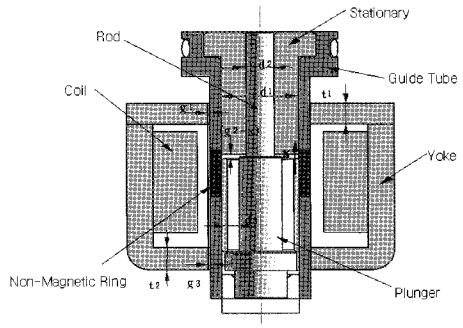

Fig. 1 Sectional diagram of the proposed solenoid actuator

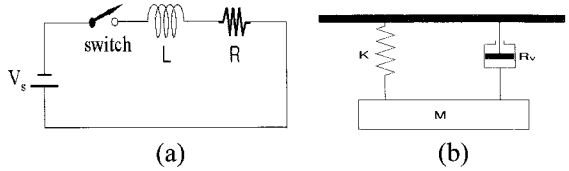

(a) (b)

Fig. 2 Equivalent circuits: (a) Electrical circuit; (b) Mechanical circuit

2.2 Characteristic Equations

In Fig. 1, g_1 is the air gap between the yoke and guide tube on the stationary side, g_2 is the air gap between the plunger and stationary, and g_3 is the air gap between the yoke and guide tube on the plunger side. If the reluctances are $\Re_1, \Re_2, \Re_3$ corresponding to each air gap, the total reluctance yields to equation (1).

$$\Re = \Re_1 + \Re_2 + \Re_3 = \frac{g_1 t_2 (d_1^2 - d_2^2 - 4d_3^2) + 4(g_2 - x) d_1 t_1 t_2 + g_3 t_1 (d_1^2 - d_2^2 - 4d_3^2)}{\mu_0 \pi d_1 t_1 t_2 (d_1^2 - d_2^2 - 4d_3^2)} \quad (1)$$

And, inductance L is to be equation (2).

$$L = \frac{N^2}{\Re} = \frac{\mu_0 \pi d_1 t_1 t_2 (d_1^2 - d_2^2 - 4d_3^2) N^2}{g_1 t_2 (d_1^2 - d_2^2 - 4d_3^2) + 4(g_2 - x) d_1 t_1 t_2 + g_3 t_1 (d_1^2 - d_2^2 - 4d_3^2)} \quad (2)$$

Electric motive force e and time varying voltage V(t) are expressed as Equations (3) and (4), respectively.

$$e = \frac{d}{dt}(L \cdot i) = L(x)\frac{di}{dt} + i\frac{dL(x)}{dx}\frac{dx}{dt} \quad (3)$$

$$V(t) = iR + L(x)\frac{di}{dt} + i\frac{dL(x)}{dx}\frac{dx}{dt} \quad (4)$$

And, the force variation according to plunger displacement is expressed as Equation (5).

$$F_{fld} = \frac{\partial \dot{W}_{fld}(i,x)}{\partial x} = \frac{1}{2} i^2 \frac{dL}{dx} \quad (5)$$

Where,

$$\frac{dL}{dx} = \frac{\mu_0 \pi d_1 t_1 t_2 (d_1^2 - d_2^2 - 4d_3^2) \cdot 4 d_1 t_1 t_2 N^2}{[g_1 t_2 (d_1^2 - d_2^2 - 4d_3^2) + 4(g_2 - x) d_1 t_1 t_2 + g_3 t_1 (d_1^2 - d_2^2 - 4d_3^2)]^2} \quad (6)$$

Referring to Fig. 2, the dynamic characteristics of the solenoid actuator can be expressed as first order differential equations (7) ~ (9) [1, 3].

$$\dot{x}_1 = x_2 \quad (7)$$

$$\dot{x}_2 = \frac{1}{M}[F_m - (\Re_v \cdot x_2) - (k \cdot x_1)] \quad (8)$$

$$\dot{x}_3 = \frac{1}{L(x_1)}\left[V(t) - x_3 \cdot \Re - x_3 \cdot \frac{dL(x_1)}{dx_1} \cdot x_2\right] \quad (9)$$

Where $x_1 (= x)$ is plunger position, $x_2 (= \dot{x})$ is plunger speed, and $x_3 (= i)$ is current.

3. Simulation and Finite Element Method(FEM) Analysis for Non-Magnetic Ring Effect

3.1 Simulation

The simulation is performed by Simulink software using equations (7)~(9) and Table 1, which are the specifications of the solenoid actuator of Fig. 1. Fig. 3 shows the simulation results for the moving characteristics of the plunger with the non-magnetic ring and without the non-magnetic ring.

Table 1 Specifications of solenoid actuator

Items	Input Voltage (V)	Coil Resistance (Ω)	Plunger Mass (g)	Stroke (mm)	Fixed Air Gap (mm)	Spring Constant (g/mm)
Spec.	DC24	20	6.15	0.95	0.05	387

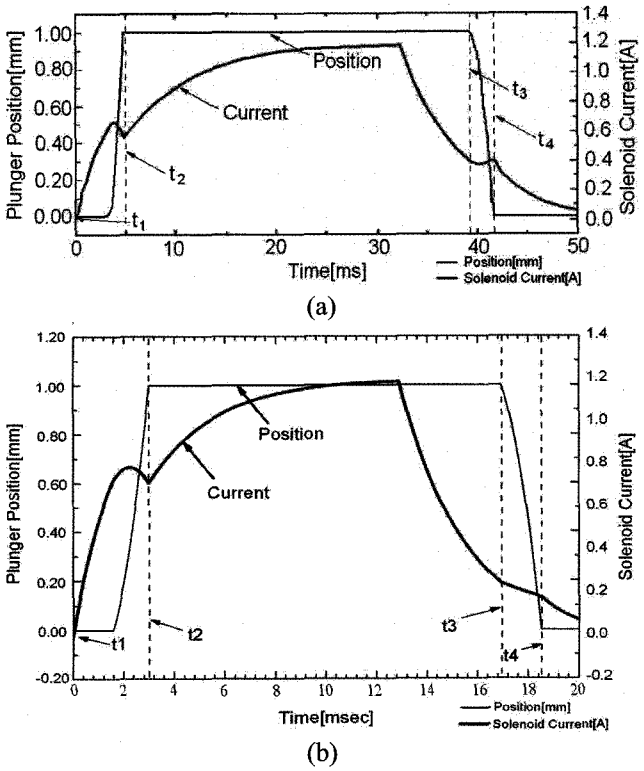

Fig. 3 Coil current and plunger position (simulation): (a) without non-magnetic ring; (b) with non-magnetic ring

In Fig. 3, the period of t_1~t_2 is the time required for plunger attraction from initial compressed position (maximum stroke) to stationary position, and t_3~t_4 is the

releasing time for the plunger returning from stationary to initial compressed position. In the current wave, the rapid increasing and decreasing period is owing to quick decreasing and increasing of reluctance according to plunger movement [1, 4-5].

For reduction of overall operating time, we can only control the attraction time by electromagnetic technique. The releasing time cannot be controlled because it is decided by return spring constant. The non-magnetic ring is also used for the reduction of attraction time.

The attraction time is 4.8ms in Fig. 3(a), which is the case without the non-magnetic ring and 3.2ms in Fig. 3 (b), which is the case with the non-magnetic ring.

We know that the attraction time can be reduced by 1.6ms due to the non-magnetic ring effect.

3.2 FEM Analysis

We can expect that the plunger speed may be affected by position and length variation of the non-magnetic ring, and we performed the FEM analysis for the purpose of examination of magnetic flux distribution in magnetic paths according to position and length variation of the non-magnetic ring. And, we decided the optimal attaching position of the non-magnetic ring on the guide tube considering the results [1, 6].

It is very difficult to sense the slight flux variation by figures representing the magnetic flux distribution using the naked eye. So, for clearer sensing of the variation of flux density in the main air gap, we added the figures representing the magnetic flux density as numerical [1, 7].

The FEM analysis was performed for the following four cases (3.2.1~3.2.4), and in each analysis, the main air gap was maintained as a full stroke of 1mm.

3.2.1 Absence of non-magnetic ring on the guide tube

This is the case in which there is only a magnetic guide tube for prohibiting the eccentric phenomenon of the plunger during movement. Fig. 4 shows the results of FEM analysis for this case.

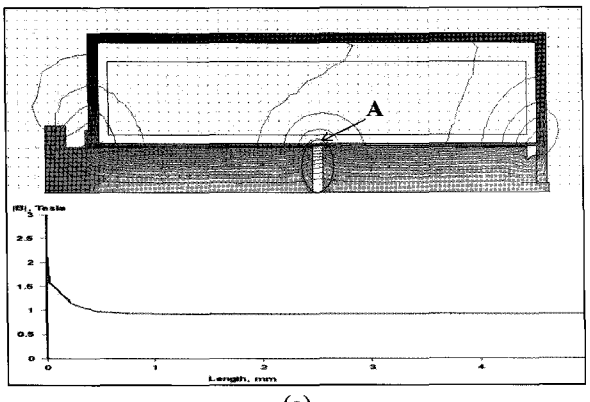

(a)

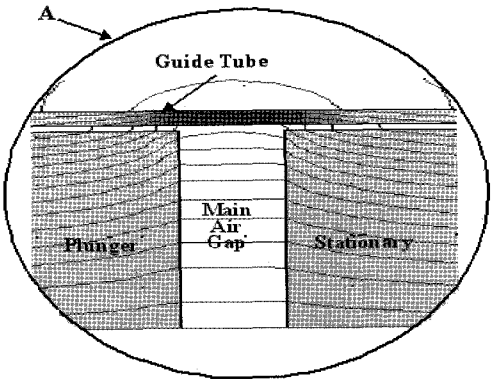

(b)

Fig. 4 Results in case in which non-magnetic ring is not used: (a) Magnetic flux distribution and density; (b) Enlargement of "A"

In Fig. 4, we can discover that the guide tube is saturated in the overlapped area with the main air gap, and the magnetic flux density in the main air gap is about 0.95[T].

3.2.2 In the case of according with centers of non-magnetic ring and main air gap

Fig. 5 shows the results of FEM analysis in the case of according with centers of non-magnetic ring and main air gap.

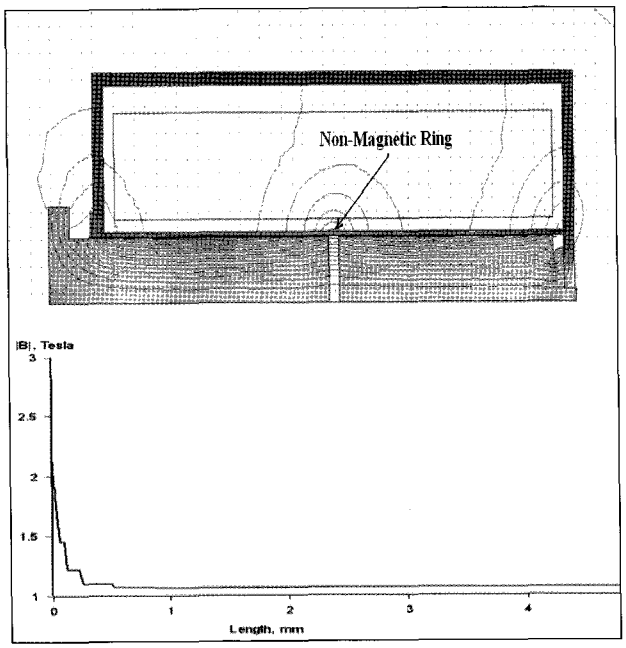

Fig. 5 Magnetic flux distribution and density in case of according with centers of non-magnetic ring and main air gap

In this case, the saturation problem in the guide tube does not arise, and the magnetic flux density is about 1.15[T], which is increased in value compared to the case in which the non-magnetic ring is not used of Fig. 4.

3.2.3 In case of inclined center of non-magnetic ring in shaft direction

Fig. 6 and Fig. 7 show the results of FEM analysis in the case of inclined center of the non-magnetic ring to the left and right side based on the center of the main air gap, respectively.

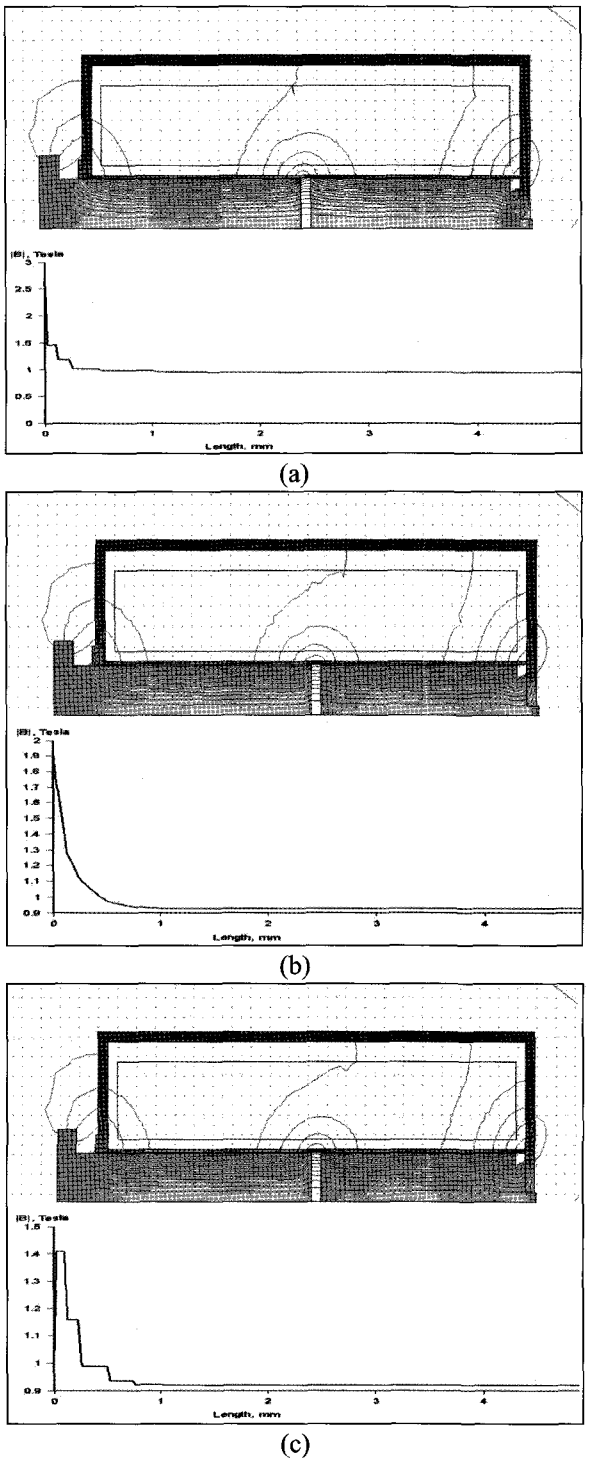

(a)

(b)

(c)

Fig. 6 Magnetic flux distribution and density in case of inclined center of non-magnetic ring to left side by: (a) 1mm; (b) 2mm; (c) 3mm

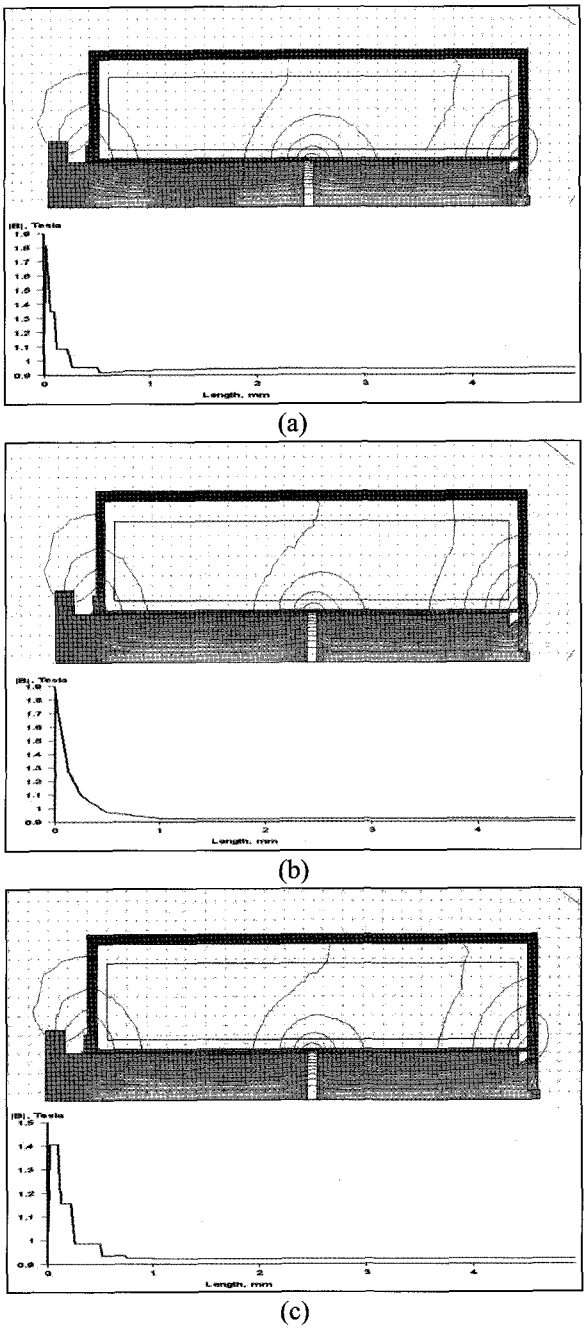

(a)

(b)

(c)

Fig. 7 Magnetic flux distribution and density in case of inclined center of non-magnetic ring to right side by: (a) 1mm; (b) 2mm; (c) 3mm

From Fig. 6 and Fig. 7, we can know that the magnetic flux densities in the main air gap are distributed by the range of 0.92[T] ~ 1[T]. This means that the magnetic flux density becomes weak compared to the case of according with centers of non-magnetic ring and main air gap (Fig. 5), and these values are similar to the value in the case in which there is no non-magnetic ring on the guide tube (Fig. 4). As it were, if the center of the non-magnetic ring is inclined to the left or right side of the center of the main air gap, the effect of the non-magnetic ring cannot be expected.

3.2.4 In case of length variation of non-magnetic ring

We can predict that the non-magnetic ring effect is arisen when the length is longer than the main air gap by consideration of the above results, but the possibility of eccentric force arising in the guide tube may be proportional to increase the non-magnetic ring length. As it were, excessive long non-magnetic ring length is meaningless for analysis. So, considering these conditions, we decided the analysis length range from 1mm to 3mm.

At this time, we changed the non-magnetic ring length maintaining the position of the center, which accorded with the center of the main air gap because the maximum magnetic flux density is produced when the centers are accorded with each other like in the result of Fig. 5.

Fig. 8 shows the results of FEM analysis in case of length variation of non-magnetic ring.

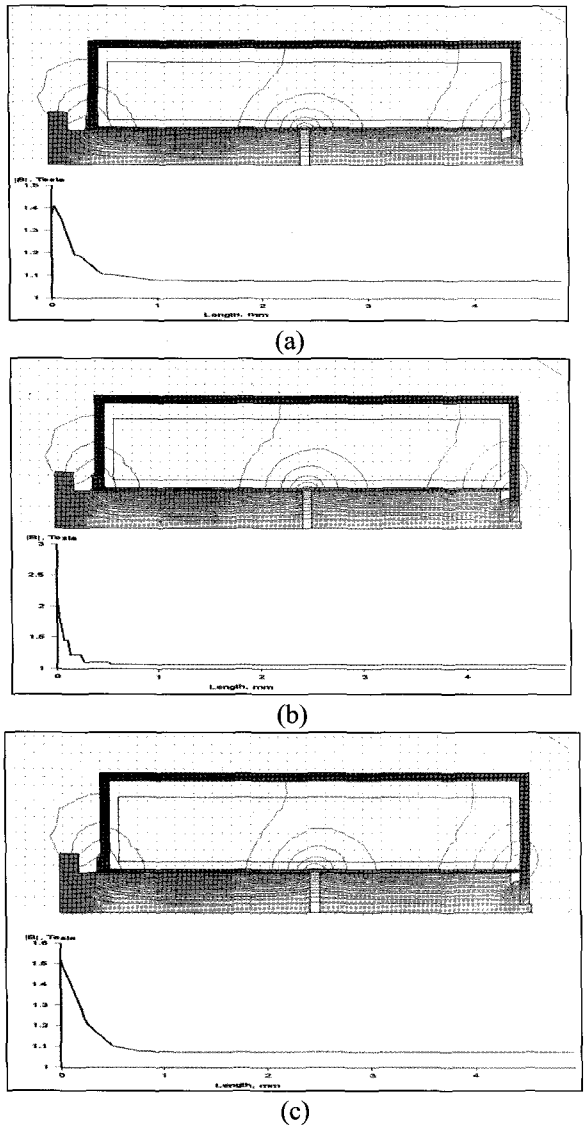

(a)

(b)

(c)

Fig. 8 Magnetic flux distribution and density in case of length variation of non-magnetic ring: (a) 1mm; (b) 2mm; (c) 3mm

The magnetic flux densities in each cases of Fig. 8 are all about equivalent to 1.1~1.15[T], which are very similar results to the case of Fig. 5.

These results suggest that the variation quantity of magnetic flux density according to the length variation of the non-magnetic ring is not significant, and for obtaining maximum flux density, the center of the non-magnetic ring should be placed at the accordance position with the center of the main air gap.

4. Manufacturing of prototype and experimental results

4.1. Manufacturing of Prototype and Experiments

The prototype actuator is made based on the specifications of Table 1, simulation results (Fig. 3), and FEM analysis (Figs. 4~8). We used soft magnetic material for composition of the magnetic circuit of solenoid actuator, having the maximum magnetic flux density is 1.5[T], which is enough to prohibit the magnetic saturation. Korean standard coil is used for the winding of the solenoid. The coil diameter is 0.25mm and turn number is 920. Experiments were performed at the Reliability Evaluation Center of the Korea Institute of Machinery & Materials by use of a general performance tester for the solenoid actuator for pneumatic valve operation.

4.2 Experimental Results

4.2.1 Operating Speed of Plunger

For this experiment, a prototype, a guide tube with a non-magnetic ring, and a guide tube without a non-magnetic ring are used. And also, an acceleration sensor is used for sensing the finishing point of the plunger attraction. Fig. 9 shows the results.

These results are similar to the simulation results of Fig. 3

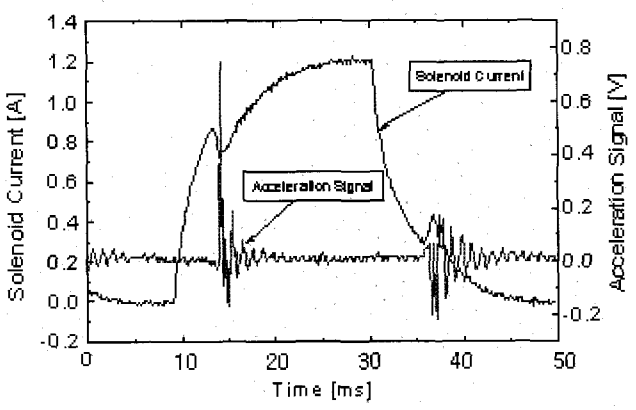

(a)

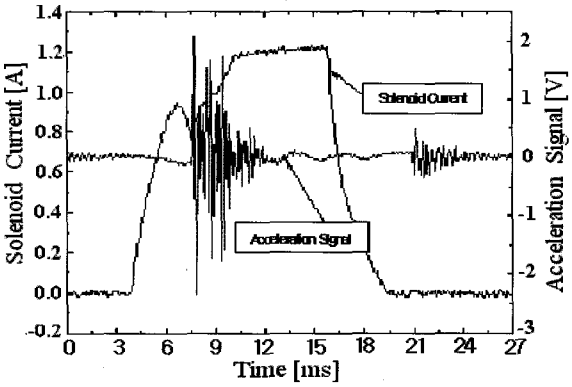

(b)

Fig. 9 Measurement results for operating time of prototype: (a) without non-magnetic ring; (b) with non-magnetic ring

even though there is a slight time difference. The attraction time of the plunger is about 5.5ms and 3.8ms in Fig. 9(a) and (b), respectively. As in the simulation, the attraction time is reduced by 1.7ms.

4.2.2 Attraction Force

We used one solenoid actuator assembly and ten guide tubes for this experiment. The attraction force is measured at three points of full stroke. Fig. 10 indicates the measurement results of attraction force for the same cases as in Figs. 4~8. Fig. 10(a) represents the result for the case in which the guide tube has no non-magnetic ring, Fig. 10(b) shows the results according to right and left variation of the center of the non-magnetic ring on the base of the center of the main air gap, and Fig. 10(c) presents the results according to length variation of the non-magnetic ring maintaining the accordance state of the center with that of the main air gap.

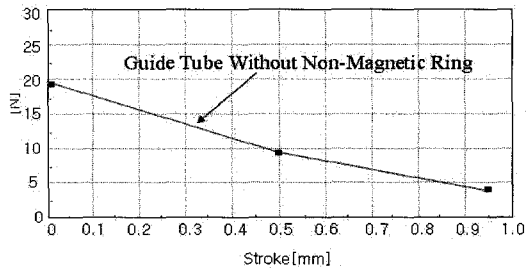

(a)

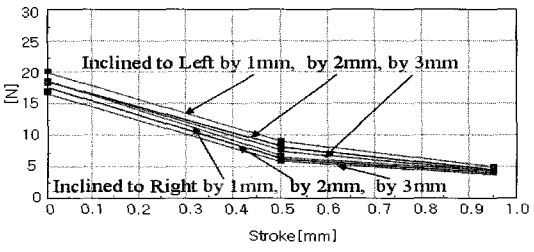

(b)

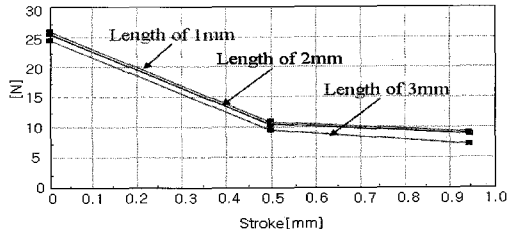

(c)

Fig. 10 Measurement results of attraction forces according to: (a) Guide tube without non-magnetic ring; (b) Position variation of non-magnetic ring; (c) Length variation of non-magnetic ring

4.2.3 Characteristics of Frequency Response

We continued the experiments until the actuator could no longer follow after the input square wave frequency. Fig. 11 shows the shape of the coil current after input frequency, and also represents that the maximum operating frequency is about 25Hz.

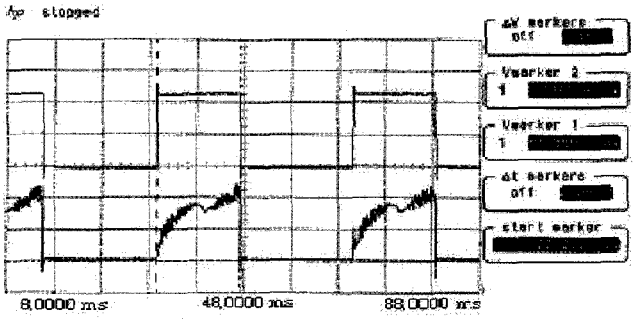

Fig. 11 Characteristics of frequency response

5. Conclusions

In this study, we performed the FEM analysis according to position and length variation of a non-magnetic ring, which is an important factor for increasing the operating speed of the solenoid actuator, and also analyzed the dynamic characteristics of the solenoid actuator by simulation and experiments.

And, we obtained the following satisfactory results:

1) From the results of FEM analyses (Figs. 4~8) and experimental results (Fig. 10), we know that the attraction force and plunger speed can be maximized when the center of the non-magnetic ring is accorded with that of main air gap, and that the influence of length variation is much less than the position variation of the non-magnetic ring.
2) The operating time of the solenoid actuator can be reduced over 30% by the proposed method in this paper.

3) In addition, we are convinced that this method can be applied to the design of the PWM controlled high-speed solenoid actuator as well as the general purpose solenoid actuator because the maximum operating frequency is 25Hz as Fig. 11 shows.

References

[1] B. J. Sung, E. W. Lee, H. E. Kim, "Characteristics of Non-Magnetic Ring for High-Speed Solenoid Actuator," The Eleventh Biennial IEEE Conference on Electromagnetic Field Computation, pp. 342, June 2004, Korea.

[2] B. J. Sung, E. W. Lee, H. E. Kim, "Empirical Design of an On and Off Type Solenoid Actuator for Valve Operation," KIEE International Sections on Electrical Machine and Energy Conversion Systems, Vol. 4B, No. 2, pp. 39~46, June, 2004.

[3] K. Hameyer and M. Nienhaus, "Electromagnetic Actuator-Current Developments and Examples," Actuator 2002 - 8th International Conference on New Actuators, pp. 170~175, 2002. 6. 10.

[4] E. M. Benavides, J. R. Perez, and R. P. Herrero, "Numerical Simulation of the Injection Process in a Two Stroke Diesel Engine," SAE Technical Paper Series, 200-01-0291, 2000.

[5] T. Kajima, S. Satoh, and R. Sagawa, "Development of High-Speed Solenoid Valve," JIEE (Part C), Volume 60, No. 576, pp. 254~261, 1994. 8.

[6] H. Roters, Electro Magnetic Device, John Wiley & Sons, Inc, 1970.

[7] Yogo, "Parameter Design of High-Speed Electro-magnetic Valve," Nachi Co., Vol. 48, No. 1, pp. 43~56, 1992.

Baek-Ju Sung

He received his B.S. and M.S. degrees in Electrical Engineering from Busan National University in 1990 and 1992, respectively. He currently works at the Korea Institute of Machinery & Materials. He is working toward a Ph. D. degree at Chungnam National University.

Eun-Woong Lee

He received his B.S., M.S., and Ph. D. degrees in Electrical Engineering from Hanyang University, Korea, in 1971, 1974, and 1983, respectively. From Mar. to Dec. 1976, he was a Faculty of the Daejon Junior Technical College.

Since 1976, he has been a Professor in the Department of Electrical Engineering, Chungnam National University, Daejon, Korea. From 1982 to 1983 and 1985 to 1986, he was a Visiting Professor in the Department of Electrical Engineering, McGill University, Montreal, Canada. From 1999 to 2002, he was Vice President and Acting President of "The Korean Federations of Teachers Associations". Now he serves as President of the "Korean Institute of Electrical Engineering (KIEE)", and Vice President of the "Korea Electric Engineers Association" and the "Korea Electric Association". His interests are in the areas of electrical machines, special purpose motors, and power quality. He has been a Senior Member of IEEE, and is a lifetime member of KIEE.